

# Operation of a Microgrid with Optimal Power Assignment at the Generation Nodes

Ariel S. Loyarte, Luis A. Clementi, Jorge R. Vega

Control and Electrical Security Group (CySE)

Department of Electrical Engineering, Santa Fe Regional Faculty (FRSF)

National Technological University (UTN)

Santa Fe, Argentina

ariel.loyarte@gmail.com; laclementi@santafe-conicet.gov.ar; jrvega@frsf.utn.edu.ar

**Abstract**—An optimization method is used for determining the electric power to be supplied at the different nodes of a microgrid with the aim of reducing generation costs, losses by electricity transmission, and greenhouse gas emissions, while simultaneously maintaining the energy quality at all points of supply. The optimization problem is complex due to the various restrictions inherent to the distributed energy resources in the microgrid. The generation sources include diesel engines, photovoltaic panels, wind turbines, and fuel cells, each of them conveniently represented by specific mathematical models. Simulation examples are presented for both island and non-island operation modes. The problem is solved through a particle swarm optimization algorithm that efficiently provides acceptable solutions.

**Index Terms**-- Distributed power generation, Microgrid, Particle swarm optimization, Power generation dispatch.

## I. INTRODUCTION

A microgrid is a low-power electrical network (e.g., less than 10 MW) that is designed to provide electricity to small towns or institutions, suburban communities, commercial and industrial areas, etc. [1]. Often, a microgrid integrates different types of distributed systems, such as small power (renewable and non-renewable) generation sources, energy storage devices, electronic control equipments, distributed loads, and protection / reconfiguration systems, with supervision and management strategies typically operated from a remote center [1,2].

In recent years, a growing effort to improve the development of microgrid systems has been observed. Many proposals aimed at efficiently covering the increasing electricity demands of users, with cheaper and safer operations than those offered by the traditional power networks. In particular, meaningful progresses have been made in the development of representative models of real networks and their various distributed resources, as well as in varying policies for establishment of buying / selling rates of the electrical energy [1-3].

A microgrid can operate in two basic modes i.e.: connected to the external power grid or isolated from it (island mode). In the first case, the microgrid can either buy or sell electricity to the external grid, to compensate for the lack (or excess) of its generation capacity with respect to the instantaneous power demand. In contrast, in island mode, the microgrid must instantaneously supply the demanded power and interact with the storage devices to compensate for the differences between the generated and demanded powers while simultaneously maintaining the electrical quality of the service in all the demand points.

The microgrid nodes are linked through electrical interconnection lines. Each node can be identified with one or more than one of the following roles: interconnection, generation, demand, and storage. Many generation resources are available, such as diesel engines, turbines, microturbines, photovoltaic panels, and fuel cells, among others. Fortunately, there are some mathematical models of those resources available in the literature [1]. In the last decade, a great advance has also been noted in the development of new devices and strategies for storing energy under different modes [4].

The global optimization of a microgrid can be stated in different ways. For example, one approach consists of determining the optimal allocation of electric powers at the different generation points in such a way that the microgrid fully covers the time-varying distributed load with a minimum global cost and a high energy quality (e.g., adequate voltage levels). In general, such problem is difficult because of the large number and diversity of involved variables and constraints. In fact, continuous, discrete, and random variables can simultaneously be present during the normal operation of a microgrid. Also, a microgrid can often suffer changes in its configuration due to connection / interconnection of electricity lines, broken connections due to short circuits, etc. In addition to the difficulties associated with the inherent physics of the electrical system, the optimal operation of a microgrid can be

conditioned by economic components related to fuel costs, undesirable gas emissions, tariff policies or differential rates. Despite the energy quality at the different network nodes should also be involved in the global optimization problem, only economic components are typical [5,6].

When the global optimization of an electric system is based on an objective function that include economic, environmental, and quality components, together with several underlying constraints, the resulting optimization problem is typically known as an Optimal Power Flow (OPF) problem. Several methodologies for the solution of OPF problems have been reviewed [7-10]. Although conventional methods are mainly based on gradient strategies, some modern techniques have the advantage of avoiding the calculation of derivatives. For example, some evolutionary search strategies, such as particle swarm optimization (PSO) algorithms [11], have proven able to efficiently solve the OPF problem within reasonable execution times [12-17].

In this work, a PSO algorithm coupled with a Newton-Raphson method is used to determine the optimal allocation of the generation powers at the different nodes of a microgrid. The simulated microgrid consists of a meshed electric network with twelve nodes, operating in either island or connected modes. The optimal operation of the microgrid is based on the simultaneous minimization of: i) the global electric generation costs, ii) the total mass flow of emitted pollutants (nitrogen oxides: NO<sub>x</sub>; carbon dioxide: CO<sub>2</sub>; and sulfur dioxide: SO<sub>2</sub>) [18], and iii) the deviation of the voltage at the load nodes with respect to their nominal values. Additionally, the optimization problem involves several technical constraints, such as limited active and reactive powers at the generation nodes, and min-max voltage tolerances at the load nodes. The considered generation sources are: diesel generators, fuel cells, and wind turbines and solar-photovoltaic parks. Functional relationships between generated power, fuel consumption, climate variables, and operative costs corresponding to each generation source were adopted from [19]. Weather conditions for Santa Fe (Argentina) were considered for quantifying the share of renewable energy sources.

## II. MATHEMATICAL MODEL OF THE MICROGRID

Consider an electrical network with  $N$  nodes ( $j = 1, \dots, N$ ). At each node  $j$ , the voltage is  $V_j$ , and the generated and consumed powers are  $S_{g,j}$  and  $S_{d,j}$ , respectively. The  $j$ -th and  $k$ -th nodes are interconnected by a transmission line of admittance  $Y_{j,k}$ . According to the microgrid structure and to the admittances of each transmission line, the following mathematical model can be written [20]:

$$(\mathbf{p} + \mathbf{q} i)^* \times [\text{diag}(\mathbf{v}^*)]^{-1} = \mathbf{Y} \times \mathbf{v} \quad (1)$$

where the first member of Eq. (1) is an  $(N \times 1)$  vector whose  $j$ -th component is the ratio  $S_j^* / V_j^* = (P_j + Q_j i)^* / V_j^*$ , being  $P_j$  and  $Q_j$  the net active and reactive powers, respectively (i.e., the difference between the generated and consumed powers in the node),  $i^2 = -1$ , and the symbol “\*” indicates complex conjugated. Also,  $\mathbf{v}$  ( $N \times 1$ ) contains the voltages  $V_j$  at the nodes; and  $\mathbf{Y}$  ( $N \times N$ ) is the matrix of nodal admittances, where its  $N^2$  admittances depend on the network configuration and on the admittances of each transmission line.

The generation nodes exhibit the following restrictions:

$$P_{g,\min,j} \leq P_{g,j} \leq P_{g,\max,j}; \quad j = 1, \dots, N_g \quad (2a)$$

$$Q_{g,\min,j} \leq Q_{g,j} \leq Q_{g,\max,j}; \quad j = 1, \dots, N_g \quad (2b)$$

Additionally, the powers of the nodes must satisfy the following relationship:

$$\sum_{j=1}^N (S_{g,j} - S_{d,j}) - S_L = 0 \quad (3)$$

where  $S_L$  is the total power that is dissipated as electric losses in the transmission lines of the whole network. Equation (3) assumes that no storage device is present in the considered microgrid.

The inverse problem known as *calculation of power flow* consists in finding  $\mathbf{v}$  in Eq. (1), from the knowledge of  $\mathbf{Y}$ , the generated active power ( $P_{g,j}$ ), and the consumed power ( $S_{d,j} = P_{d,j} + Q_{d,j} i$ ), at each node  $j$ . This is true for all but one  $j$  node; i.e., the so-called slack bus, where the complex voltage is known and the powers are unknown.

## III. MODELS FOR THE GENERATION SOURCES

The generation sources considered in the microgrid are: 2 diesel generators, 1 fuel cell generator, 1 wind farm, and 1 solar-photovoltaic park. In what follows, static generation models for each electric source are presented. Such models describe: 1) the generation costs in terms of the produced active powers, in the cases of the diesel and fuel cell generators; and 2) the generated active powers in term of weather conditions, in the cases of the wind and solar parks.

### III.1. Diesel Generator

The operative cost (i.e., the cost per energy unit) of a diesel generator (DG) can be represented by the following quadratic polynomial in the generated active power [19]:

$$C_{\text{DG}} = \alpha P_{g,\text{DG}}^2 + \beta P_{g,\text{DG}} + \gamma \quad (4)$$

where  $P_{g,DG}$  is the active power generated by the DG, and the constant parameters  $\{\alpha, \beta, \gamma\}$  are obtained on the basis of a fuel consumption test and from the diesel fuel cost.

### III.2. Fuel Cell

For modeling the fuel cell (FC) generator, it is assumed that a steam reforming system is used to obtain hydrogen from natural gas. Thus, the operative cost of a FC generator ( $C_{FC}$ ) includes the costs specifically invested for the FC operation ( $C_{op,c}$ ) and for the steam production ( $C_{op,s}$ ). Then, the  $C_{FC}$  can be calculated as follows:

$$C_{FC} = (C_{op,c} + C_{op,s}) P_{g,FC} \quad (5)$$

where  $P_{g,FC}$  is the active power generated by the FC. In this work, a constant efficiency of 80% was adopted for the steam generator. More detailed models for  $C_{op,c}$  and  $C_{op,s}$  are available [21].

### III.3. Photovoltaic Generator

For known weather conditions, the photovoltaic (PV) panels generate the active power  $P_{g,PV}$ , which can be calculated as follows:

$$P_{g,PV} = N_{g,PV} P_{peak} \frac{G}{G_{std}} [1 + k_p (T - T_r)] \quad (6)$$

where  $N_{PV}$  is the number of PV panels in the park,  $P_{peak}$  is the peak-power of a single panel,  $G$  (W/m<sup>2</sup>) is the solar irradiance,  $T$  (°C) is the ambient temperature,  $k_p$  is the temperature-power coefficient (typically provided by the panel manufacturer),  $G_{std}$  (= 1000 W/m<sup>2</sup>) is the reference irradiance, and  $T_r$  (= 25 °C) is the reference temperature. The operative cost of the PV generator was not considered because the cost of maintenance is practically negligible.

### III.4. Wind Turbine

The operative cost of the whole wind farm was neglected. The active power  $P_{g,WT}$  generated by the wind farm is obtained as follows:

$$P_{g,WT} = \frac{1}{2} N_{WT} C_p \rho A v \quad (7)$$

where  $N_{WT}$  is the number of wind turbine (WT) generators in the park,  $C_p$  is the power coefficient of a single turbine,  $\rho$  is the air density,  $A$  is the rotor area, and  $v$  is the wind velocity.

## IV. OPTIMIZATION OF THE MICROGRID

Consider a general case where both the network structure ( $N$ ,  $N_g$ , and  $Y$ ) and the distribution of powers in the load nodes

( $S_{d,j} = P_{d,j} + Q_{d,j} i$ ) are known. The problem consists in determining the voltage levels ( $V_{g,j}$ ) and the active powers ( $P_{g,j}$ ) to be injected into each generation node, in order to satisfy a predetermined optimal operating condition. For example, a feasible objective function ( $f$ ) to be minimized can include terms of emission of pollutants by the generators, the deviation of the voltages with respect to limiting quality levels, the cost of the consumed fossil fuels, and the transmission losses, among other possible factors.

At the generation nodes, the vectors  $\mathbf{p}_g$  and  $\mathbf{v}_g$  represent the active powers and the voltages, respectively. Then, the optimization problem can be stated as follows:

$$\min_{\mathbf{p}_g, \mathbf{v}_g} f(\mathbf{p}, \mathbf{q}, \mathbf{v}) \quad (8)$$

subject to:

$$P_{g,\min,j} \leq P_{g,j} \leq P_{g,\max,j}; \quad j = 1, \dots, N_g \quad (9a)$$

$$q_{g,\min,j} \leq q_j \leq q_{g,\max,j}; \quad j = 1, \dots, N_g \quad (9b)$$

$$V_{\min,j} \leq V_j \leq V_{\max,j}; \quad j = 1, \dots, N \quad (9c)$$

$$\sum_{j=1}^{N_g} (P_{g,j} - P_{d,j}) - P_L = 0 \quad (9d)$$

$$\sum_{j=1}^{N_g} (q_{g,j} - q_{d,j}) - q_L = 0 \quad (9e)$$

Traditional gradient descent algorithms are inapplicable to solve the previous optimization problem, because: i) the functional  $f$  cannot normally be expressed in a differentiable form (due to the inclusion of the term that accounts for the voltage deviations in the load nodes); and ii) the solution space typically exhibits multiple local minima. In contrast, stochastic search algorithms tend to be more suitable to deal with this kind of problems. For example, genetic algorithms or particle swarm optimization (PSO) algorithms could be evaluated as feasible computational tools. Unfortunately, these evolutionary algorithms are incapable for ensuring the convergence to the global solution.

A PSO algorithm can be used to find an approximation to the optimal solution corresponding to Eqs. (8, 9) through a set of evolutionary particles. Each particle represents a possible solution of the problem; and the whole particle swarm moves over the solution space until a stable state is found. The  $p$ -th particle in the swarm represents a point in the  $(N_g + N_g) \times 1$  space, i.e.  $\mathbf{X}^p = [\mathbf{p}_g^p \quad \mathbf{v}_g^p]$ . The best position obtained by the  $p$ -th particle is  $\mathbf{P}^p$ , and the best historical position obtained by the

whole swarm is  $\Gamma$ . Also, the  $p$ -th particle moves over the solution space with a velocity  $\mathbf{V}^p [(N_g+N_g) \times 1]$ . The swarm is initialized at the first iteration; and then, at the  $n$ -th iteration, the position and velocity of each particle are updated according to [11]:

$$\mathbf{V}^p[n+1] = w[n] \mathbf{V}^p[n] + c_1 R_1[n] \{\mathbf{B}^p - \mathbf{X}^p[n]\} + c_2 R_2[n] \{\Gamma - \mathbf{X}^p[n]\} \quad (10a)$$

$$\mathbf{X}^p[n+1] = \mathbf{X}^p[n] + \mathbf{V}^p[n+1] \quad (10b)$$

where  $w[n]$  is the inertia;  $c_1$  and  $c_2$  are the cognitive and social accelerations, respectively; and  $R_1[n]$  and  $R_2[n]$  are two random values chosen at each iteration from a uniform distribution in the interval (0,1). The total number of iterations is chosen to ensure the convergence of the PSO algorithm, and  $\Gamma$  is adopted as the final solution.

## V. SIMULATION EXAMPLE

Consider a microgrid of  $N = 12$  nodes with the configuration sketched in Fig. 1. The network geometry and the physical characteristics of the interconnection electric lines were used to calculate the nodal admittance matrix  $\mathbf{Y}$  ( $12 \times 12$ ), on the basis of three (coplanar horizontal) aluminum conductor steel-reinforced of  $35/6 \text{ mm}^2$ , a base power of 1,000 kVA, and a base voltage of 13.2 kV. Matrix  $\mathbf{Y}$  is not here presented due to space reasons. However, it is important to highlight that the condition number of  $\mathbf{Y}$  (i.e., the ratio between the largest and the lowest singular values) is  $\approx 1.7 \times 10^5$ , thus indicating the ill-conditioning degree of the associated optimization problem [22]. All the power profiles corresponding to the base day are shown in Fig. 2, with data available at intervals of 1 hour. Average active and reactive powers are respectively 46.1 kW and 40.6 kVAr, for residential loads (RL); and 102.0 kW and 63.2 kVAr, for industrial loads (IL).

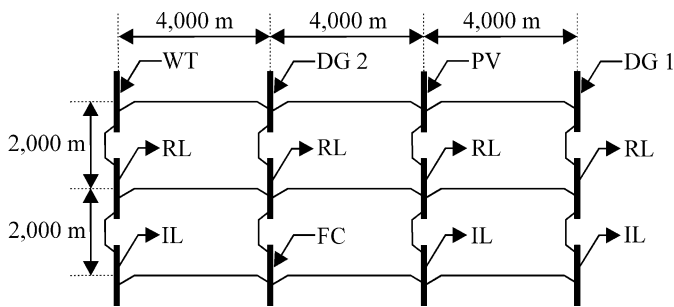


Figure 1. Scheme of the simulated microgrid.

The electric powers  $P_{g,PV}$  and  $P_{g,WT}$  of Fig. 2a were calculated through Eqs. (6, 7), respectively, from the climatic conditions corresponding to a (summer) base day (January 1, 2013), which were provided by the Meteorological Information

Center (Santa Fe, Argentina). Both renewable sources were assumed to mainly generate active power, with minima (inductive or capacitive) power factors of 0.97 (typical values of standard inverter devices).

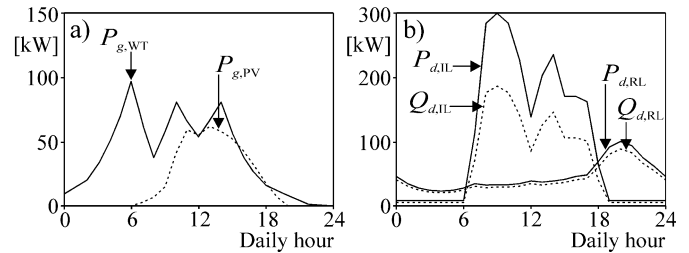


Figure 2. a) Renewable generation ( $\approx 100\%$  of active power); b) Total (active and reactive) power demands in the microgrid.

The  $N_g = 5$  ‘generation nodes’ include: 2 diesel generators (DG 1: 850 kW, DG 2: 800 kW); 1 fuel cell (FC: 300 kW); 1 park of 500 photovoltaic panels (PV:  $100 \text{ W} \times 500$ ); and 1 park of 40 wind turbines (WT:  $2 \text{ kW} \times 40$ ). The  $N_d = 7$  ‘load nodes’ are characterized by their load curves: 4 (identical) RL curves, of  $P_d = 100 \text{ kW}$  and  $Q_d = 90 \text{ kVAr}$ ; and 3 (identical) IL curves, of  $P_d = 300 \text{ kW}$  and  $Q_d = 190 \text{ kVAr}$ , where  $P_d$  and  $Q_d$  are the maxima active and reactive powers, respectively. Curves for active power demand are scaled from those purposed in [23], by considering inductive power factors of 0.75 and 0.85, for RL and IL, respectively.

In the present work, the function  $f$  is defined by the following expression:

$$f(\mathbf{p}, \mathbf{q}, \mathbf{v}) = k_1 C(\mathbf{p}_g) + k_2 E(\mathbf{p}_g) + k_3 D(\mathbf{v}, \mathbf{p}_g) \quad (11)$$

where  $C(\mathbf{p}_g)$  is the global generation cost (basically, the fuel costs for the two DG and the FC);  $E(\mathbf{p}_g)$  depends on the mass flow of released pollutants ( $\text{NO}_x$ ,  $\text{CO}_2$ ,  $\text{SO}_2$ ); and  $D(\mathbf{v}, \mathbf{p}_g)$  is the average voltage deviations at the load nodes with respect to their nominal values.  $C(\mathbf{p}_g)$ ,  $E(\mathbf{p}_g)$  and  $D(\mathbf{v}, \mathbf{p}_g)$  are normalized functions whose minima would be zero. The weight factors  $\{k_1, k_2, k_3\}$  can be chosen with the aim of prioritizing fuel consumption, pollutant emissions, or quality of the electrical service. The cost  $C(\mathbf{p}_g)$  is calculated through Eqs. (4, 5), while the emissions  $E(\mathbf{p}_g)$  are calculated as in [19]. In the case of renewable sources, environmental pollution is neglected.

The optimal assignment of powers at each generation node is obtained by solving Eqs. (8, 9). The optimization was implemented at intervals of 1 hour, using a PSO with 50 particles and  $w = c_1 = c_2 = 0.5$ . In general, a stable solution for  $f$  was achieved in around 50 iterations. Figure 3 shows the results at 12, 17, and 21 hours. Comparison of the 3 figures at  $n = 1$  only indicates the random initialization of the PSO. Although not shown, the voltages at all delivery points reached adequate

values. In all cases, it is observed that the PSO algorithm was effective for reducing  $f$  (Fig. 3d). The optimal assignment of powers verify:  $P_{g,DG2} > P_{g,FC} > P_{g,DG1}$ . However, the power ratios are different in the three cases, and therefore the optimum solution is not obvious. Table 1 summarizes the optimal powers that must be assigned at each generation node.

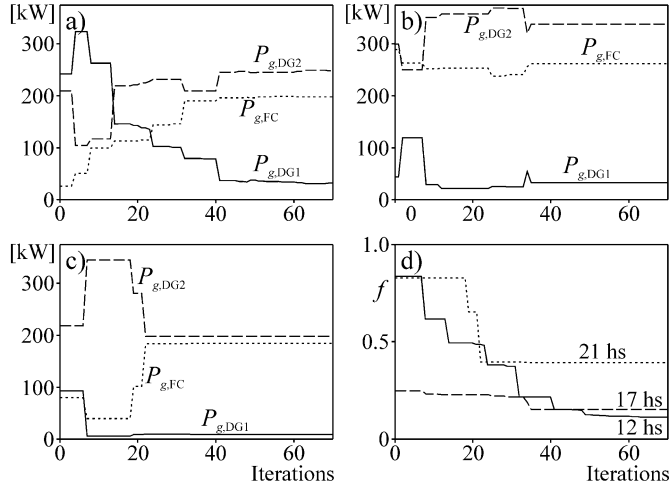


Figure 3. Estimated active powers by the PSO algorithm at different iterations ( $n$ ): a) 12 h., b) 17 h., c) 21 h. d) Evolution of the objective function  $f$  ( $k_1=0.7$ ,  $k_2=0.2$ ,  $k_3=0.1$ ) with increasing values of  $n$ .

Table 1: Optimal power assignments at the generation nodes (percentages per generation source are indicated between parentheses).

	12 h.	17 h.	21 h.
$P_{g,DG1}$ (kW)	26.3 (5.5%)	32.0 (5.1%)	8.4 (2.2%)
$P_{g,DG2}$ (kW)	245.7 (51.5%)	337.6 (53.5%)	197.7 (50.7%)
$P_{g,FC}$ (kW)	205.2 (43.0%)	261.1 (41.4%)	183.7 (47.1%)

As a consequence of the ill-conditioning of matrix  $\mathbf{Y}$  in Eq. (1), the solution of the optimization problem of Eq. (7) is highly sensitive to small changes in the load profiles. For instance, Table 2 compares the active powers injected by DG 1, DG 2, and FC, at 12 hours of the analyzed base day with the new optimal solution when the power loads were modified as follows: (i) the powers of 2 RL were increased by 2.5%, and the two remaining RL were decreased by 2.5%; and (ii) the powers of 2 IL were increased by 2.5%, and the third IL was decreased by 2.5%. Despite the relatively small changes in the power loads ( $\approx 2.5\%$ ), the optimal powers were significantly modified (see Table 2). Moreover, with this alternative loads, the FC (instead of DG 2) should have to provide the largest power to the microgrid.

## VI. CONNECTION TO THE EXTERNAL GRID

Assume that a node is able to import electricity from the distribution network. The maxima active and reactive powers to be imported by such a node are limited to 300 kW and  $\pm 300$  kVar, respectively. For simplicity, we also assume that the function  $f$  only considers the generation costs. Call  $C_{FC}$  and  $C_{DG}$  ( $> C_{FC}$ ) the costs of FC and DG generation, respectively; and  $C_{imp}$  the cost of importing an electric power,  $P_{imp}$ . Then, three cases were numerically analyzed (see results in Table 3): (A)  $C_{imp} > C_{DG}$ ; (B)  $C_{FC} \approx C_{imp} < C_{DG}$ ; and (C)  $C_{imp} < C_{FC}$ . In case (A), the algorithm reproduces identical results to those of the ‘island-mode’. In such case,  $P_{g,DG2} = 8.0$  kW corresponds to the lowest admissible power for a DG, while  $P_{g,FC} = 300$  kW corresponds to the maximum capacity of the FC. In case (B), a large  $P_{imp}$  is preferred due to the large costs involved in the diesel generation; and  $P_{g,DG1}$  suffers a noticeable reduction. In Case (C), the imported power practically reaches the maximum of 300 kW, which suggests the convenience of a greater energy importation. In this case, the contributions from the 2 diesel generators are small, and the FC reduced its contribution to almost a 50%. All these simulations clearly suggest that the second DG could be discarded. In such a case, a new solution should be sought.

Table 2: Comparison of optimal power assignments at 12 h. for the base day and for an alternative load with disturbances of  $\approx 2.5\%$  in the loads.

	Base day	Alternative load
$P_{g,DG1}$ (kW)	26.3 (5.5%)	36.9 (7.8%)
$P_{g,DG2}$ (kW)	245.7 (51.5%)	169.3 (35.7%)
$P_{g,FC}$ (kW)	205.2 (43.0%)	267.5 (56.5%)

Table 3: Optimal power assignments at 12 h. for island mode, and comparison with three different non-island modes (A, B, C).

	‘Island mode’	(A)	(B)	(C)
$P_{g,DG1}$ (kW)	169.2	169.2	29.0	44.1
$P_{g,DG2}$ (kW)	8.0	8.0	12.0	9.2
$P_{g,FC}$ (kW)	300.0	300.0	297.5	133.8
$P_{imp}$ (kW)	-	0.0	138.7	290.2

## VII. CONCLUSIONS

The proposed optimization algorithm was able to efficiently establish a load dispatch policy at the available generation nodes. It is apparent that the results will depend on the selected functional  $f$  and the weighting factors assigned to each of their terms.

Although not here shown, the PSO algorithm was evaluated on the basis of several loading states and initial conditions, and proved to be efficient to find repetitive solutions. The algorithm was implemented on a standard personnel computer, and the observed computation times reached several minutes. This extent of simulation times is acceptable provided that the microgrid operate under slow variations in the electric load distributions among the different nodes.

The size and the configuration of the microgrid directly affect the matrix  $\mathbf{Y}$ , and consequently the numerical conditioning of the optimization problem. As a consequence, small changes in the distributed loads can induce meaningful changes in the optimal power assignments. For this reason, efficiency of the optimization algorithm is important for thinking in a feasible online implementation.

The connection to the external grid suggests different power assignments that depend on the comparison between the costs of the imported energy and the global generation costs in the microgrid. Again, a faster optimization algorithm would be useful for keeping an optimal operation of the microgrid under a possible time-varying tariff policy, as usual in modern electric markets.

#### ACKNOWLEDGMENT

We are thankful to the National Technological University (UTN), for supporting this research through the research Project code ENUTIFE0002405TC. Also, we thank to the Meteorological Information Center (CIM) of the National University of the Litoral (Santa Fe, Argentina) for providing us with data of temperatures, winds, and solar irradiances over Santa Fe city.

#### REFERENCES

- [1] S. Chowdhury, S. P. Chowdhury and P. Crossley, *Microgrids and Active Distribution Networks*, Herts: The Institution of Engineering and Technology, 2009, p. 1.
- [2] D. Zhang, "Optimal Design and Planning of Energy Microgrids", Ph.D. Thesis, University College London, 2013.
- [3] E. Kremers, P. Viejo, O. Barambones and J. González de Durana, "A Complex Systems Modelling Approach for Decentralised Simulation of Electrical Microgrids", in *Proc. 2010 15<sup>th</sup>. IEEE Int. Conf. on Eng. of Complex Comp. Syst.*, pp. 302-311.
- [4] C. Naish, I. McCubbin, O. Edberg, M. Harfoot, "Outlook of Energy Storage Technologies", Policy Department Economy and Science, Bruxelles, Tech. Rep. IP/A/ITRE/FWC/2006-087/Lot 4/C1/SC2, Feb. 2008.
- [5] J.Y. Kim, H.S. Lee and J.H. Park, "A Modified Particle Swarm Optimization for Optimal Power Flow", *Journal of Electrical Engineering & Technology*, vol. 2(4), pp. 413-419, 2007.
- [6] P.K. Roy, S.P. Ghoshal and S.S. Thakur, "Biogeography Based Optimization Approach for Optimal Power Flow Problem Considering Valve Loading Effects", *International Journal on Recent Trends in Engineering & Technology*, vol. 3(3), pp. 177-181, 2010.
- [7] R.V. Amarnath and M.V. Ramana, "State of art in optimal power flow solution methodologies", *Journal of Theoretical and Applied Information Technology*, vol. 30(2), pp. 128-154, 2011.
- [8] K.S. Pandya, and S.K. Joshi, "A survey of optimal power flow methods", *Journal of Theoretical and Applied Information Technology*, vol. 4(5), pp. 450-458, 2008.
- [9] S. Frank, I. Steponavice and S. Rebennack, "Optimal Power Flow: A Bibliographic Survey I", *Energy Systems*, vol. 3(3), pp. 221-258, 2012.
- [10] M.R. AlRashidi and M.E. El-Hawary, "Applications of computational intelligence techniques for solving the revived optimal power flow problem", *Electric Power Systems Research*, vol. 79(4), pp. 694-702, 2009.
- [11] Y. Shi and R. Eberhart, "A Modified Particle Swarm Optimizer", in *Proc. 1998 IEEE Conf. on Evolut. Comput.*, pp. 69-73.
- [12] M. R. AlRashidi and M. E. El-Hawary, "A Survey of Particle Swarm Optimization Applications in Electric Power Systems", *IEEE Trans. on Evol. Comp.*, vol. 13, pp. 913-918, 2009.
- [13] Dieu Ngoc Vo and P. Schegner, *Meta-Heuristics Optimization Algorithms in Engineering, Business, Economics, and Finance - Chapter 1: An Improved Particle Swarm Optimization for Optimal Power Flow*, IGI Global, 2013.
- [14] S. He, J.Y. Wen, E. Prempain, Q.H. Wu, J. Fitch and S. Mann, "An improved particle swarm optimization for optimal power flow", *International Conference on Power System Technology (PowerCon)*, vol. 2, pp. 1633-1637, 2004.
- [15] P. Oñate Yumbra, "Solución del problema de flujos de potencia óptimo con restricciones de seguridad por un optimizador de partículas modificado", Thesis, Centro de Investigación y de Estudios Avanzados del I.P.N., Guadalajara (México), 2008.
- [16] M. R. AlRashidi, M. F. Alhajri, and M. E. El-Hawary, "Enhanced particle swarm optimization approach for solving the non-convex optimal power flow", *World Academy of Science, Engineering and Technology*, vol. 62, pp. 651-655, 2010.
- [17] J.Y. Kim, H.S. Lee and J.H. Park, "A Modified Particle Swarm Optimization for Optimal Power Flow", *Journal of Electrical Engineering & Technology*, vol. 2(4), pp. 413-419, 2007.
- [18] W. Morgantown, "Emission Rates for New DG Technologies", The Regulatory Assistance Project, May 2001: <http://www.raonline.org/document/download/id/66>.
- [19] F. Mohamed, "Microgrid Modelling and Online Management", Ph.D. Thesis, Helsinki University of Technology, 2008.
- [20] J. Grainger and W. Stevenson, *Análisis de Sistemas de Potencia*, Naucalpan de Juarez: McGraw-Hill, 1996, p. 223.
- [21] M.I. Sosa, J.L. Silveira and A. Fushimi, "Natural Gas Steam Reforming for Hydrogen Production - An Exergetic Approach", *Proceedings of the 5th Latin-America Congress: Electricity Generation and Transmission CLAGTEE*, Paper B-150, pp. 1-10, 2003.
- [22] R. Aster, B. Borchers and C. Thurber, *Parameter Estimation and Inverse Problems*, Whaltham: Elsevier Academic Press, 2005, p. 1.
- [23] J.A. Jardini, C. Tahan, M.R. Gouvea, Se Un Ahn and F.M. Figueiredo, "Daily Load Profiles for Residential, Commercial and Industrial Low Voltage Consumers", *IEEE Transactions on Power Delivery*, vol. 15(1), pp. 375-380, 2002.